BEST: International Journal of Management, Information Technology and Engineering (BEST: IJMITE)
ISSN 2348-0513
Vol. 2, Issue 7, Jul 2014, 85-92

STRUCTURAL AND OPTICAL STUDIES OF CuO DOPED POLYANILINE

SUSHEEL KUMAR SINGH[1], ARVIND KUMAR VERMA[2], RAM LAKHAN[3] & R. K. SHUKLA[4]

[1,2,4]Department of Physics, University of Lucknow, Lucknow, Uttar Pradesh, India

[3]Department of Physics, Eritrea Institute of Technology (EIT), Eritrea, North East Africa

ABSTRACT

Polyaniline/CuO composites at different weight percentages are synthesized by chemical oxidative polymerization method. The composites have been synthesized with various compositions (10, 15, and 20 wt %) of cupric oxide in PANI, the chemical characterization are made using XRD (X-ray diffraction), FT-IR (Fourier transform spectroscopy), UV–vis (ultra-violet visible spectrophotometer), The PL(Photoluminescence spectroscopy) techniques confirms the synthesis of the polyaniline and CuO doped polyaniline composite. The surface morphology of these composites is studied with scanning electron micrograph (SEM).

KEYWORDS: Conducting Polyaniline, XRD, SEM, FTIR, UV-Visible, PL, Nanocomposites Polyaniline

INTRODUCTION

Conducting polymers have a wide range of application areas such as rechargeable batteries, organic field effect transistors, sensors, plastic solar cells and anticorrosive materials due to their unique physical and chemical properties.[1-12] Generally, polymers are known as a class of heat sensitive, flexible, electrically insulating and amorphous or semi crystalline materials. The electrical properties of polymers can be modified by the addition of inorganic materials. Nanoscale particles as fillers are attractive due to their intriguing properties arising from the nanosized and resulting large surface area. The doping of nanoscale materials may improve the electrical and dielectric properties of the host polymers.[13] Among the various conducting polymers, polyaniline (PANI) has received great attention due to its simple preparation, environmental stability, interesting redox behaviour and tunable electro-optical properties.[14-17] The electrical properties of conducting polymer could be modified by the addition of inorganic fillers.[18-21] In the present work, chemically synthesized PANI as emeraldine powder form are characterized by XRD, SEM, FTIR and UV-visible spectroscopy. Dielectric properties of prepared samples are investigated in details. To the best of our knowledge, structural and dielectric properties of PANI/CuO is thoroughly reported in the present work at higher frequency. Dielectric measurements are carried out as function of temperature and frequency.

METHODS

Aniline hydrochloride (2.59 g) was dissolved in distilled water in a volumetric flask to make 50 mL solution. Ammonium peroxydisulfate (5.71 g) was dissolved in water also to make 50 mL of solution. Both the solutions were kept for 1 hour at room temperature. They were then mixed with a brief stirring and left at rest to polymerize. The solution turned to dark green within few minutes. Next day PANI Precipitate was collected on a filter paper, washed three times with 100 mL portions of 0.2 M HCl to remove the uncreated aniline and its oligomers from the precipitate. After this process, precipitate was washed in three times with 100 mL portions of acetone to absorb the water molecules and for the removal of any residual organic impurities. PANI, synthesized by this method, is formed in its protonated state. The precipitate was firstly dried in air for 30 min and then in oven for 3 hours at 60 ^{0}C. The synthesized PANI was ground in form of fine powder. Pellets were prepared by compressing the powder under a pressure of 10 tons with the help of a

hydraulic press machine. All the pellets were annealed at 100 ^{0}C for one hour. The thickness of the pellets of sample was found to be 3 mm. The diameter of the pellets was found to be 13 mm.

CHARACTERIZATIONS

The XRD spectra of all the samples recorded by PANalytical, X'pert PRO diffractometer using CuKα radiation (λ=1.54056 A^o) were presented for structural analysis of the samples.. FTIR spectra of all the samples in the form of powder were recorded on the Bruker Alpha spectrometer to determine the formation of polyaniline. To record absorbance spectra, 0.02 g of each sample is dissolved in 5 mL of m-cresol. Then the absorption spectra of the solutions thus formed were recorded with UV–Vis spectrophotometer (Model No.V-670 Jasco). The PL spectra of the all samples were taken by Photoluminescence spectrophotometer (LS-55, Perkin Elmer).

RESULTS AND DISCUSSIONS

X-Ray Diffraction

XRD spectra recorded for the sample a, b, and c and curves a, b, and c correspond to 0, 10, and 20 wt% CuO doped PANI composites, respectively. Polyaniline is inherently amorphous and hence there are no sharp peaks for Polyaniline. The X-Ray diffraction pattern, Figure 1(a) indicates that strongly disordered, the PANI shows only a small scattering around 2θ = 15.53.[22, 23] The crystalline nature of nano-composites are determined from XRD analysis. The XRD patterns of pure polyaniline and PANI/CuO nano-composites are shown in Figure 1 a, b and c respectively. The main peaks in the XRD pattern of pure PANI are observed at 2θ = 15.53^0 and the other characteristic peaks ascertained from the XRD pattern of PANI/CuO nano-composites are at 2θ = 35.54^0, 38.71^0, 48.94^0. The diffraction peaks at 2θ values of 35.54^0, 38.71^0 and 48.94^0 corresponding to (-1 1 1), (1 1 1) and (-2 0 2) Miller planes are selected for calculating the crystallite size for CuO phase. Similar result of CuO are earlier reported by Abd El-Aziz A.Said et al.[24] Crystallite size can be estimated from the full width at half maximum (FWHM) of the X-ray diffraction data. The broadening of the FWHM is inversely proportional to the average crystallite size, D, as predicted by the well-known Scherer's formula.[25] The crystallite size, D, is calculated from the following relation:

$$D = k\lambda/\beta \cos\theta \quad (1)$$

where, λ, is the X-ray wavelength; k, the shape factor; D, the average diameter of the crystals in angstroms; θ, the Bragg angle in degree; and β is the line broadening measured by half-height in radian. The value of k depends on several factors including the miller index of the reflection plane and the shape of crystal. If the shape is unknown, k is often considered to be 0.89. The crystallite size of PANI/CuO nano-composites are formed to lies between 15-45 nm.

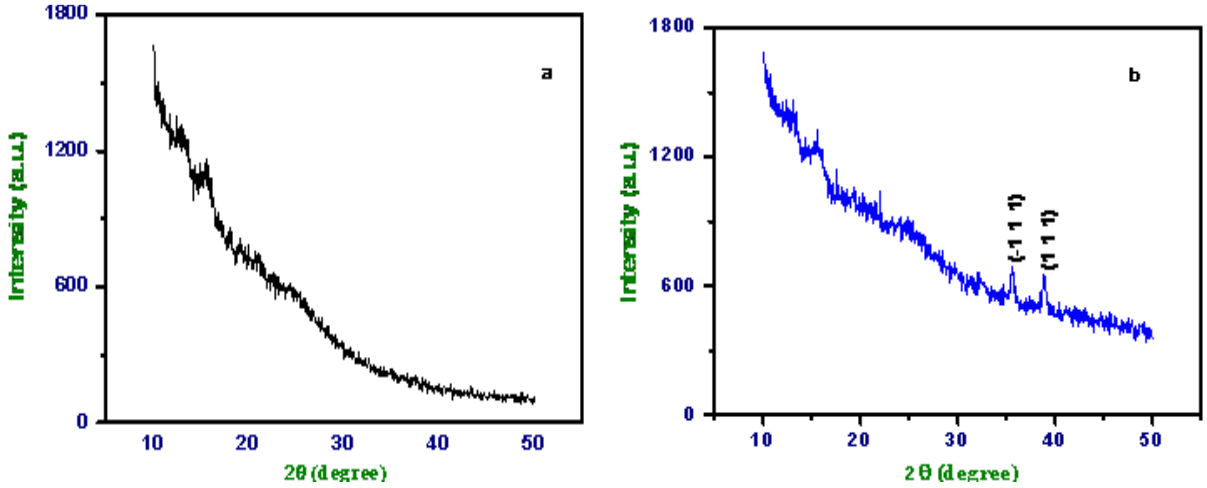

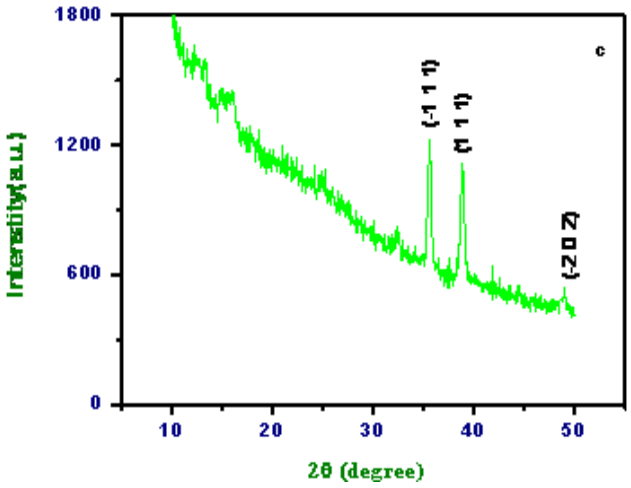

Figure 1: XRD Spectra for the Sample a, b, and C and Curves a, b, and c Correspond to 0, 10, and 20 Wt% CuO Doped PANI Composites, Respectively

Scanning Electron Microscopy

The morphology of pure PANI and PANI/CuO nanocomposites are studied by using scanning electron microscopy (SEM). SEM images of pure polyaniline and PANI/CuO nanocomposites synthesized shown in Figure 2 (a-d) corresponds 0, 10, 15 and 20 wt % CuO doped PANI composite respectively. SEM image of pure PANI shown in Figure 2 (a) tends to aggregate in large particles in the form of large globules, which are not same for PANI/CuO nanocomposites samples shown in Figure 2 (b-d). The globules structure formation in the polyaniline takes place due to heterogonous nucleation, as a result of smooth continuous flat like structure are formed. However, the absence of pores in the structure shows that very strong interactions occur among the particles.

Conductivity is provided by the mobility of charge carriers in such structures, which is closely related to interparticle interactions. It is, therefore, reasonable to conclude that PANI/CuO nanocomposites are conductive. Figure 2 (b-d) show that the structure of PANI/CuO nanocomposites are more homogeneous with increased wt% of CuO doped PANI composite, particle size decreased and homogeneity increased, by chemically adsorption to the polymer, and prevented from preventing undesirable grass particles with a narrower particle size dispersion and brighter image (i.e. the noise is reduced) than for its undoped counterpart. The greater brightness is due to the higher efficiency of electrons originating from the samples surfaces, which is attributed to higher conductivity of doped-PANI sample.

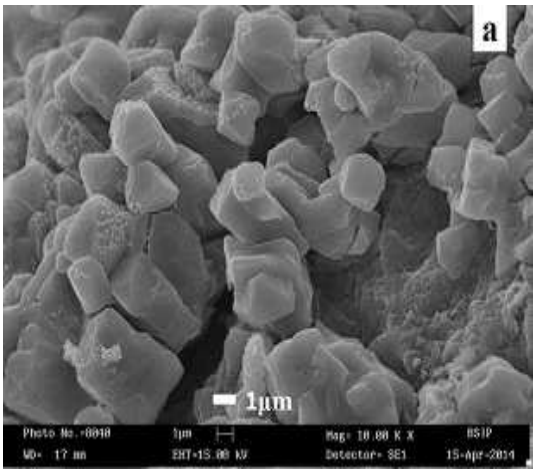

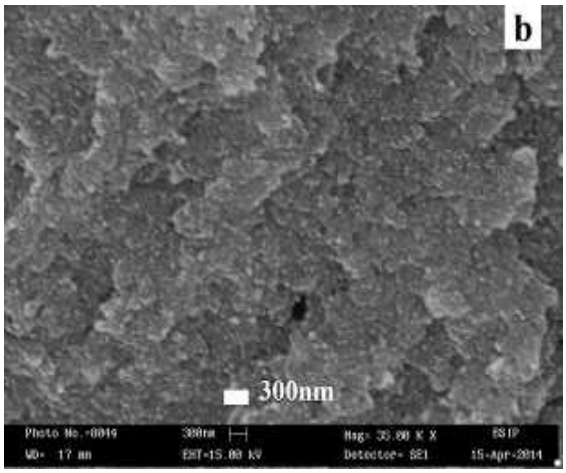

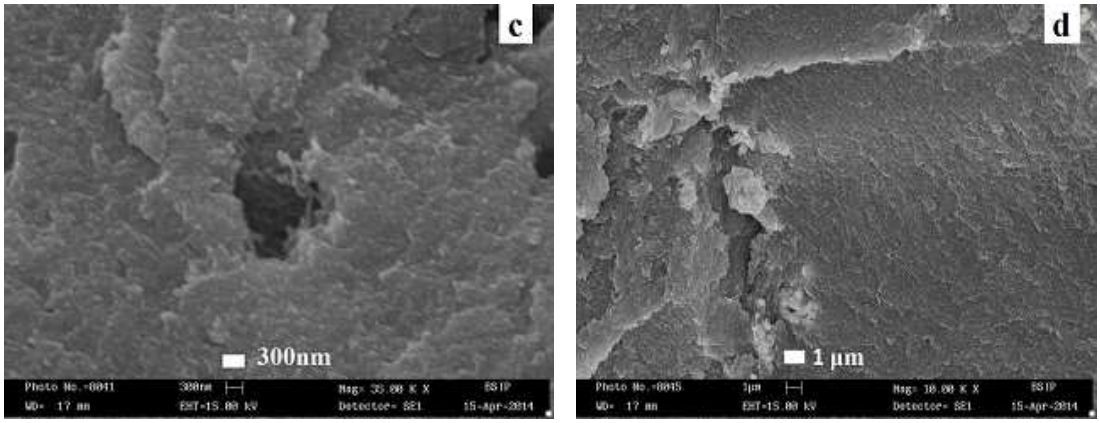

Figure 2: SEM Images of Samples a, b, c, and D and Images a, b, c and D Correspond to 0, 10, 15 and 20 Wt% CuO Doped PANI Composite, Respectively

FTIR Analysis

FTIR spectra of all the samples of pure PANI and PANI/CuO nanocomposites at different wt% are obtained in the absorbance range 400–4000 cm^{-1} which are shown in Figure 3. The vibrational bands observed for pure PANI and PANI/CuO nanocomposites are explained on the basis of normal modes. FTIR Spectra of all the samples of pure PANI and PANI/CuO nanocomposites show strong absorption bands, in the region 740–1650 cm^{-1} which correspond to the characteristics of polyaniline. The absorbance band at around 752 cm^{-1} observed for pure PANI and PANI/CuO nanocomposites samples show characteristics peaks of the C-H out-of plane bending vibration of the 1, 4-distibuted benzene ring.[26] The strong intensity bands at 869 cm^{-1} (as in pure PANI) is assigned to C-H out of plane bending vibration of the (1, 2, 4 trisubstituted) benzene ring deformation.[27], which shifted to splitted bands at 906 cm^{-1} in 10 wt%, 916 cm^{-1} in 15 wt% and 927 cm^{-1} in 20 wt% CuO doped PANI composite. The observed peaks around 1220 cm^{-1} for pure PANI and PANI/CuO nanocomposites is C- N stretching → C- C stretching.[28] And observed peaks around 1393 cm^{-1} for pure PANI and PANI/CuO nanocomposites can be attributed to torsion C-N oscillations in the alkyl chain.[29] The absorption peaks observed around 1630 cm^{-1} for all Pure PANI and PANI/CuO nanocomposites are attributed to C=C stretching in aromatic nuclei.[30] The observed peaks around at 2422 cm^{-1}, 3688 cm^{-1} and 3796 cm^{-1} for the pure PANI and different weight percentage of PANI/CuO nanocomposites can be probably related to the valence oscillation of the C-H and N-H bond stretching within the benzene rings, which have been associated with electrical conductivity and high degree of electron delocalization PANI. The splitting and intensity of absorption band on increasing the CuO weight percentage [Figure 3 (b-d)] suggest the presence of higher extent of protonation in these samples. This interpretation also finds support from electrical measurements studies.

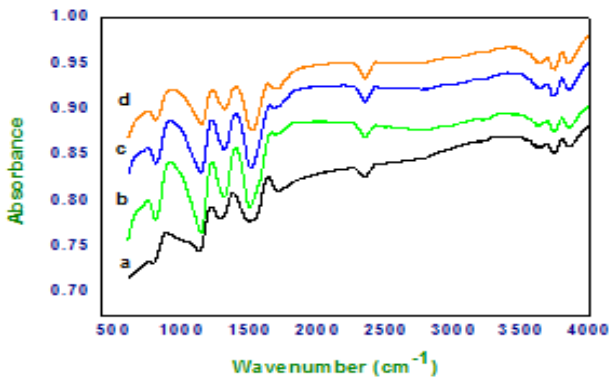

Figure 3: FTIR Spectra for the Sample a, b, c, and d Curves a, b, c, and D Correspond to 0, 10, 15 and 20 Wt% CuO Doped PANI Composite, Respectively

UV-Vis Spectrum

The UV–vis absorption spectra of the pure PANI and the PANI/CuO nanocomposites are recorded at room temperature by using a spectrophotometer between the wavelength range 200–800 nm as shown in Figure 4. Optical spectroscopy is an important technique to understand the conducting states corresponding to the absorption bands of inter and intra gap states of conducting polymers.[31] Figure 4 illustrates the major absorption peaks at 300 nm and 440 nm. The observed bathochromic shift at the intense band 300 nm is due to the π-π* transition of benzenoid ring which is related to the extent of conjugation between the adjacent phenylene rings in the polymeric chain and the forced planarization of π -system induced by aggregation.[32] It leads to increased conjugation and thus lowers the band gap.[33], which is well agreed with the band gap result obtained in the polyaniline. The transition of π-π* of benzenoid ring and the formation of polaron band in the nanocomposites are responsible for increase of the electrical conductivity of the nanocomposite.[34] The peak at 440 nm is due to polaron- transition and shift of electron from benzenoid ring to quinonoid ring.[35] Figure 4 demonstrates the high intense blue shift of absorption peaks of PANI from its actual position in PANI/CuO nanocomposites which indicates that the addition of CuO filler particles in the polyaniline matrix has large influence on absorption spectra in the PANI/CuO nanocomposites. As seen in Figure 4 a, b, c and d as the dopent percentage increases the absorbance peaks is decreases due to Hypochomic effect. The difference between the two spectra is due to the presence of an electron withdrawing sulfonic group in the complex and therefore the transition band is observed at a lower wavelength. The absorption of the polaron band is strongly dependent on the molecular weight of the polymer.[36]

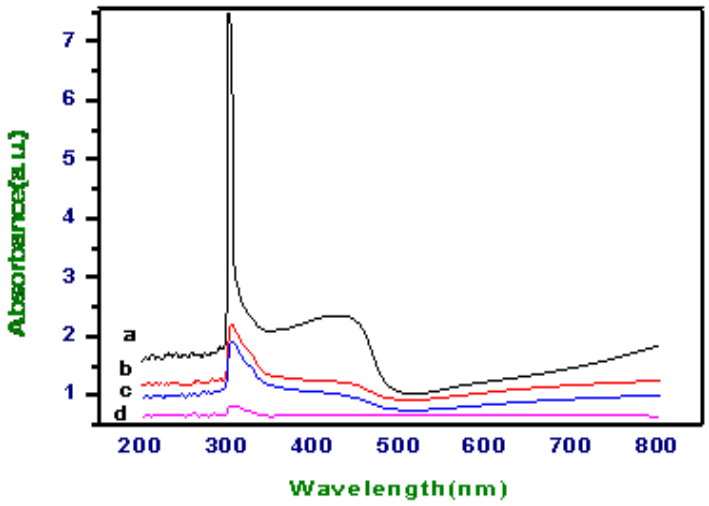

Figure 4: UV–Vis Absorption Spectra for the Samples a, b, c and d at Room Temperature, Curves a, b, c and d Correspond to 0, 10, 15, and 20 Wt % CuO Mixed PANI Composite, Respectively

Photoluminescence Studies

Photoluminescent organic molecules are a new class of compounds with interesting properties. They undergo emission over a wide range from the violet to the red. They can also be combined in several different forms to produce white light. One category of organic material with photoluminescence properties is conjugated organic polymers. PL spectra were measured for all the four samples in the range of 200 - 800 nm and the wavelength of excitation chosen for all the samples is 243 nm. The photoluminescence spectroscopy (PL) of CuO doped PANI has been performed and is shown in Figure 5. The PL spectra of 0, 10, 15, and 20 wt% CuO doped PANI samples show peaks in visible emission around at 399 nm in violet region, 480 nm in blue region, and 530 nm in green region. One of the related PL peaks have been reported, the PL spectra of CuO observed the NBE at 395 nm in the violet Region[37]. The relative heights of the emission peaks alter with different dopant concentrations and nature of solvents (due to polarity). It has been noticed

that the peak observed at 399 nm in undoped PANI small shifts towards higher wavelength with increased wt% CuO. In addition, this peak becomes sharp and intense. This may be due to interchain species which plays an important role in the emission process of conjugated polymers. The intensity of peaks depends on factors such as polymer coil size, the nature of polymer-solvent, polymer-dopant interactions, and the degree of chain overlapping[38]**.** The PL spectra of samples have the same shape, which indicates that it is an efficient way to tune the intensities of the peak by employing specific dopant with different wt%. The observed reduced height of the photoluminescence emission intensity peaks with increased wt% CuO doped PANI might due to the possibility of atoms/molecules of dopant (CuO) forming aggregation in the polymer chain[39]. Overall, it is clear that the nature of conjugated polymer aggregation depends upon many factors, including the polymer coil size, the nature of polymer–solvent and polymer–dopant interactions and the degree of chain overlap. The PL spectra of the samples have the same general shape, which indicates that it is an efficient way to tune the intensities of the peak by employing dopant at different concentration levels.

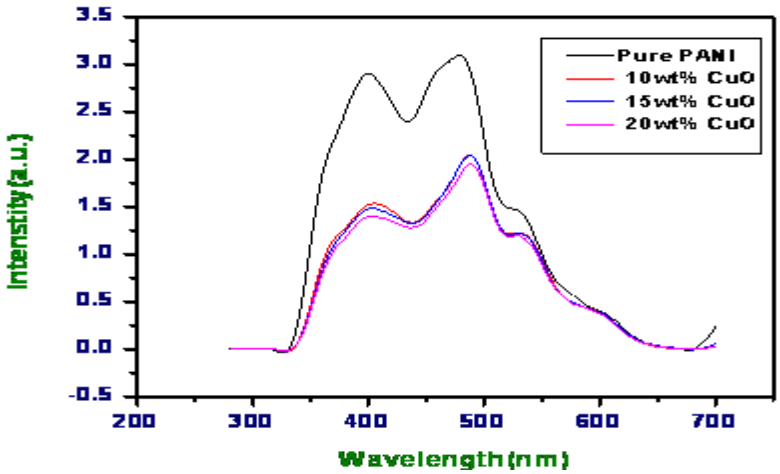

Figure 5: Photoluminescence Spectra for the Samples A, B, C and D at Room Temperature, Curves A, B, C and D Correspond to 0, 10, 15, and 20 Wt % CuO Mixed PANI Composite, Respectively

CONCLUSIONS

We have synthesized pure and CuO doped PANI nanocomposite by the chemical oxidation method at room temperature. The prepared samples have been characterized by XRD, SEM, and FTIR. XRD spectra show the crystalline quality of all the samples, whereas the PANI synthesized is amorphous in nature. The study of FTIR spectra confirms the formation of conducting PANI and also suggests that doped of CuO in PANI does not affect its structure. The UV–Vis absorption spectra of the solutions of all the samples contain two major peaks at 300 nm and 440 nm. The observed bathochromic shift at the intense absorption band 300 nm is due to the π-π* transition of benzenoid ring which is related to the extent of conjugation between the adjacent phenylene rings in the polymeric chain and the forced planarization of π -system induced by aggregation and the absorption peak at 440 nm is due to polaron-transition and shift of electron from benzenoid ring to quinonoid ring. The PL spectra of pure and PANI/CuO nanocomposites samples show peaks in visible emission around at 399 nm in violet region, 480 nm in blue region, and 530 nm in green region. In this work it has been noticed that the peak observed at 399 nm in pure PANI small shifts towards higher wavelength with increased wt% CuO. In addition, this peak becomes sharp and intense. This may be due to interchain species which plays an important role in the emission process of conjugated polymers. The PL spectra of samples have the same shape, which indicates that it is an efficient way to tune the intensities of the peak by employing specific dopant with different wt%. The observed reduced height of the photoluminescence emission intensity peaks with increased wt% CuO doped PANI might due to the possibility of atoms/molecules of dopant (CuO) forming aggregation in the polymer chain.

SEM images of pure PANI show to aggregate in large particles in the form of large globules structure, which are not same for PANI/CuO nanocomposite samples. The globules structure formation in the polyaniline takes place heterogonous nucleation. As a result smooth continuous flat like structure are formed in the PANI/CuO nanocomposites.

ACKNOWLEDGEMENTS

The authors are grateful to Dr. R.K. Tiwari and Dr. K.K. Verma, Center of Excellent, Department of physics and Electronics, Dr. R.M.L. Awadh University for providing XRD facility.

REFERENCES

1. H.Zengin, G.Kalayc (2010**),** Mater. Chem. Phys, 120, 46
2. S. Sinha, S. Bhadra, D. Khastgir (2009), J. Appl. Polym. Sci, 112, 3135.
3. W. Shen, M. Shi, M. Wang, H. Chen (2010), Mater. Chem. Phys, 122, 588.
4. *S*. Kazim, V. Ali, M. Zulfequar, M. M. Haq, M. Husain (2007**),** Curr. Appl. Phys, 7, 68.
5. A**.** Sarkar, P. Ghosh, A. K. Meikap, S.K. Chattopadhyay, S.K. Chatterjee,. K. Roy, B. Sah, (2008), J. Appl. Polym. Sci., 108, 2312.
6. S. De, A. Dey, S.K. De (2005), Eur. Phys. J., 46, 355.
7. D.K. Pradhan, R.N.P. Choudhary, B.K. Samantaray **(**2009), Mater. Chem. Phys**.,** 115, 557.
8. E. Ozkazanc, S. Zor, H. Ozkazanc, U. Abaci (2011), Polym. Eng. Sci., 51, 617.
9. P. Dutta, S. Biswas, S.K. De (2002), Mater. Res. Bull., 37, 193.
10. A. Drury, S. Chaure, M. Kroll, V. Nicolosi, N. Chaure, W.J. Blau (2007), Chem. Mater., 19, 4252.
11. Q. Tang, J. Wu, X. Sun, Q. Li, J. Lin (2009), Langmuir, 25, *5253.*
12. K. Singh, A. Ohlan, R.K. Kotnala, A.K. Bakhshi, S.K. Dhawan (2008), Mater. Chem. Phys., 112, 651.
13. A. Dey, S. De, A. De, S. K. De (2004), Nanotechnology, 15, 1277.
14. E. M. Genies, A. Boyle, M. Lapkowski, C. Tsintavis **(**1990) Synth. Met**.**, 36, 139.
15. P. Alexander, N. Ogurtsov, A. Korzhenko, G. Shapoval (2003**),** Prog Polym. Sci., 28, 1701.
16. N. V. Blinova, J. Stejskal, M. Trchova, J. Prokes, M. Omastova (2007), Eur. Polym. J., 43, 2331.
17. N. Gospodinova, L. Terlemezyan (1998), Prog. Polym. Sci., 23, 1443.
18. A. Dey, S. De, A. De, S. K. De (2004), Nanotechnology, 15, 1277.
19. J. H. Sung, H. J Choi, (2005), J. Macromol. Sci. B: Phys., 44, 365.
20. W. J. Bae, K. H. Kim, W. H. Jo (2004), Macromolecules, 37, 9850.
21. A. Sarkar, P. Ghosh, A. K. Meikap, A. K. Chattopadhyay, A. K. Chatterjee, M. Ghosh (2006), J. Phys. D: Appl. Phys., 39, 3047.
22. D. L. Wise, G. E. Wnek, D. J. Trantolo, T. M. Cooper, and J. D. Gresser (1996**)**, Marcel Dekker, Inc., New York.
23. H. Eisazadeh **(**2007) Journal of Applied Polymer Science, Vol.: 3, 104.

24. A.E.A. Said, M.A.E. Mohamed, A.S. Soliman, M.N. Goda (**2**014**)**, Nanoscience and Nanoengineering, 17-28.

25. H. P. Klug, and L. E. Alexander, **(**1974**)**, Polycrystalline and Amorphous Materials, 2nd Edition, Wiley-VCH, Vol.:1, pp 992.

26. S.K. Shukla, A. Bharadvaja, A. Tiwari, G.K. Parashar, G.C. Dubey (2010), Adv. Mat.Lett, DOI: 10.5185/amlett., 5127.

27. M. Trchov an J. d Stejskal (2011), Pure Appl. Chem., Vol.: 83, No. 10, pp. 1803-1817.

28. S. Khasim, S. C. Raghavendra, M. Revanasiddappa and M.V.N. Ambika Prasad (2005**)** Ferroelectrics, 325, 111–119.

29. P. Stackhira, V. Cherpak, D. Volynyuk, Z. Hotra, V. Belukh, O. Aksimentyeva, B. Tsizh and L. Monastyrskyi (2010), Rev. Adv. Mater. Sci., 23, 180-184.

30. J. Vivekanandan, V. Ponnusamy, A. Mahudeshwaran, and P.S. Vijayanand (2011), Arch. Appl. Sci. Res., 3, 6, 147-153.

31. M. K. Ram, O. Yavuz, V. Lahsangah, and M. Aldissi (2005), Sensors and Actuators B, vol.: 106, no. 2, pp. 750–757.

32. K. Gopalakrishnan, C. Ramesh, M. Elango and M. Thamilselvan (2014), ISRN Materials Science Volume 2014, Article ID 567927.

33. S. D. D. V. Rughooputh, S. Hotta, A. J. Heeger and F. Wudl (1987), Journal of Polymer Science B, vol.: 25, no. 5, pp. 1071–1078.

34. D. Y. Godovsky, A. E. Varfolomeev, D. F. Zaretsky (2001), Journal of Materials Chemistry, vol.: 11, no. 10, pp. 2465–2469,

35. A. G. Mac Diarmid and A. J. Epstein (1994), Synthetic Metals, vol.: 65, no. 2-3, pp. 103–116.

36. M. R. Nabid and A.A. Entezami (2004), Journal of Applied Polymer Science, Vol.: 94, 254–258.

37. N. Mukherjee, B. Show, S.K. Maji, U. Madhu, S.K. Bhar, B.C. Mitra, G.G. Khan, A. Mondal (2011), Mater. Lett., 65, 3248-3250.

38. S. Ameen, V. Ali, M. Zulfequar, M. Mazharul Haq and M. Husain (2007), J. Polym. Sci. Part B: Polym. Phys., 21 265.

39. Sadia Ameen, Vazid Ali, M. Zulfequar, M. Mazharul Haq, M. Husain (2009), Journal of Applied Polymer Science, Vol.: 112, 2315–2319